

Many-body mobility edge in a quasi periodic system

Sabyasachi Nag and Arti Garg

Condensed Matter Physics Division, Saha Institute of Nuclear Physics, 1/AF Bidhannagar, Kolkata 700 064, India

We analyze many body localization (MBL) in an interacting quasi-periodic system in one-dimension. We explore effects of nearest-neighbour repulsion on a system of spin-less fermions in which below a threshold value of quasi-periodic potential $h < h_c$, the system has single particle mobility edge at $\pm E_c$ while for $h > h_c$ all the single particle states are localized. We demonstrate based on our numerical calculation of participation ratio in the Fock space and Shannon entropy, that both for $h < h_c$ and $h > h_c$, the interacting system can have many-body mobility edge. For $h < h_c$, if the system is away from half-filling such that the Fermi energy in non-interacting case is below $-E_c$ and single particle states below and around the Fermi-energy are localized, then the corresponding interacting system shows MBL for a set of low energy many body states ($E < E_1$) for weak to intermediate values of interaction. The states in the middle of the many body spectrum are delocalised while the very high energy states $E > E_2$ are localized. As the interaction strength increases, more states in the many body spectrum get delocalised. On the other hand for $h < h_c$ if the system is at half filling, such that in the non-interacting case Fermi energy lies in-between $\pm E_c$ and single particle states around the Fermi energy are extended, then even the interacting system remains delocalised and does not show MBL for any strength of interaction. We also studied the energy resolved entanglement entropy and eigenstate thermalisation hypothesis (ETH) in this system and found that the low energy many body states, which show area law scaling for entanglement entropy also do not obey ETH. The crossings from volume to area law scaling for entanglement entropy and from thermal to non-thermal behaviour occurs at characteristic energies $\tilde{E}_1 < E_1$ and $\tilde{E}_2 > E_2$ indicating that Shannon entropy and participation ratio in Fock space overestimates the extend of localized regime. For $h > h_c$ where all the single particle states are localized, for $h \sim h_c$ a fraction of single particle states are still weakly localized. In this limit, the interacting system has many-body mobility edge with states in the middle of the many body spectrum $E_1 < E < E_2$ being delocalised while states below E_1 and above E_2 are localised. For very large strength of quasi-periodic potential $h \gg h_c$, for which all the single particle states are strongly localized, weak to intermediate strength of interaction is not sufficient to delocalize any of the many body states and the entire spectrum shows MBL.

PACS numbers: 72.15.Rn, 05.30.Fk, 05.30.Rt

INTRODUCTION

Interplay of disorder and interactions in quantum systems is a topic of great interest in condensed matter physics. According to the seminal work by Anderson, in a non-interacting disordered system quantum-interference among impurity scattered paths might result in a diffusion-less situation [1] due to localization. In one and two dimensions, any small amount of randomness is sufficient to localize all the single particle states while in three dimensions there occurs a single particle mobility edge leading to a metal-Anderson Insulator transition as a function of the disorder strength [2]. The question of immense interest, that has remained unanswered for decades after Anderson's work, is what happens to Anderson localization when both disorder and interactions are present in a system. Recently Basko et. al. [4] based on their perturbative treatment of interactions have established that Anderson localization can survive interactions and disordered many body eigenstates can localize resulting in a many body localized (MBL) phase, provided that interactions are sufficiently weak while strong interactions can destroy localization, resulting in a MBL

transition. Followed up by this work, MBL transition has also been established non perturbatively in lattice models with finite energy density where it can extend all the way up to infinite temperatures [5, 6].

The MBL phase and the MBL transition are unique for several reasons and challenge the basic foundations of quantum statistical physics [7, 8]. A hallmark of MBL is its non-ergodicity. In the MBL phase the system explores only an exponentially small fraction of the configuration space and local observables do not thermalize leading to violation of eigenstate thermalisation hypothesis (ETH) [9–11]. MBL phase has been shown to have similarity with integrable systems [12, 13] with an extensive number of local integrals of motion [14, 15]. Recently a lot of progress has been made in the field based on numerical analysis of interacting one dimensional models of spin-less fermions or spins with completely random disorder [16–18] as well as models where there is no randomness but have a quasi-periodic potential [19–21]. An example of such model is Aubry-Andre (AA) model [22] which has a quasi-periodic potential and even in 1-d it shows a localization to delocalization transition. Interacting version of this model has been shown to have a

MBL to delocalisation transition [19].

In this work we consider a generalized AA model [23] which has been shown to have a tunable single particle mobility edge at $\pm E_c$ for the strength of quasiperiodic potential $h < h_c$ while all the single particle states are localized for $h > h_c$. This model was studied recently [20] but to the best of our knowledge energy resolved analysis necessary to answer the question related to the existence of a many body ME was not done. We analyse the effect of interactions on this model for $h < h_c$ as well as for $h > h_c$ and ask the question is there a many body mobility edge in this system. Earlier, many works have indicated towards the existence of a many body-mobility edge at finite energy density in the spectrum [21, 24, 25] consistent with the fact that conductivity remains zero even at finite temperature in a MBL system [4].

Main findings of our work based on exact diagonalisation of this model, presented in the phase diagram of Fig. 1, are following: (1) For $h < h_c$, where there is a single particle ME, it is possible to have a many body ME for some parameter set. If in the non interacting system Fermi energy $-E_c < \epsilon_F < E_c$ such that states around ϵ_F are extended, then even in the presence of interactions this system remains delocalised and never shows MBL. (2) But for $h < h_c$ with system less than half-filled such that in the non interacting system $\epsilon_F < -E_c$, then even in the presence of interactions, many body states in the low energy part $E < E_1$ and very high energy part $E > E_2$ of the spectrum are localized while the intermediate energy $E_1 < E < E_2$ states are delocalised. (3) For $h > h_c$ but very close to h_c even at half filling, the interacting system shows MEs at the bottom and top of the many body spectrum while for $h \gg h_c$, all the many body states show MBL for weak to intermediate strength of interactions resulting in an infinite temperature MBL phase. (4) The characteristic energy scales E_1 and E_2 are obtained based on analysis of normalized participation ratio (NPR) in the Fock space and Shannon entropy. Based on crossover from volume to area law scaling of the entanglement entropy (EE) we get another set of mobility edges \tilde{E}_1 and \tilde{E}_2 such that many body states $E < \tilde{E}_1$ and $E > \tilde{E}_2$ have area law scaling of EE while for $\tilde{E}_1 < E < \tilde{E}_2$, EE obeys volume law scaling. (5) Considering ETH, we found that for $E < \tilde{E}_1$ and $E > \tilde{E}_2$, ETH is not obeyed while the intermediate energy region $\tilde{E}_1 < E < \tilde{E}_2$ is thermal. (6) Further, we demonstrated that $E_1 > \tilde{E}_1$ and $E_2 < \tilde{E}_2$ which indicates that NPR analysis overestimates the region of MBL phase.

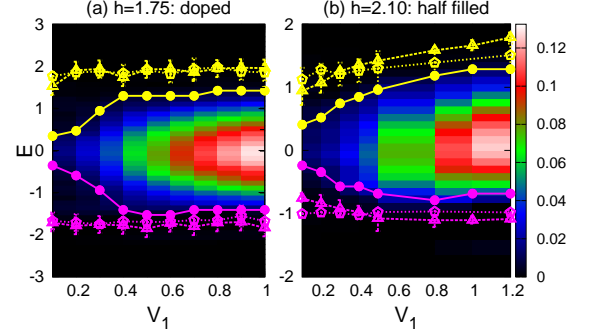


FIG. 1: Phase diagram for model in Eq. 2 in E (the energy density) and V_1 plane. Left panel shows the phase diagram for $h = 1.75$ quarter filled case while the right panel shows the phase diagram for half filled $h = 2.1$ case. We have shown the value of $\eta(E)$ in the thermodynamic limit as a function of V_1 . The curves joining the full dots represent the mobility edges $E_{1,2}$ obtained from the scaling of NPR and Shannon entropy, while the curves joining diamonds and triangles represent the mobility edges $E_{1,2}$ obtained from the energy resolved entanglement entropy and the ETH respectively. For the many body states below E_1 and above E_2 , fraction of states contributing in the Fock space vanishes in the thermodynamic limit. States below \tilde{E}_1 and above \tilde{E}_2 show area-law for Renyi entropy and do not obey ETH while the states in the middle of the spectrum $\tilde{E}_1 < E < \tilde{E}_2$ show volume law for Renyi entropy and also obey ETH.

MODEL

The model we study is a generalized Aubry-Andre (AA) model of the form $H = H_0 + H_{in}$ with:

$$H_0 = -t \sum_i [c_i^\dagger c_{i+1} + h.c.] + \sum_i h_i n(i) \quad (1)$$

$$H_{in} = V_1 \sum_i n(i)n(i+1) \quad (2)$$

Here t is the nearest neighbour hopping amplitude for spin-less fermions on a one dimensional chain, h_i is the on site potential of quasi periodic form $h_i = h \cos(2\pi\alpha i^n + \phi)$ where α is an irrational number and ϕ is an offset. V_1 is the strength of repulsion between nearest neighbour fermions. Note that $n = 1$ for $V_1 = 0$ corresponds to AA model which has all single particle states localized for $h < 2t$ and all the states are delocalised for $h > 2t$. But for $n < 1$ and for $V_1 = 0$, Hamiltonian in Eq. 2 is known to have a single particle mobility edge at $E_c = \pm[2t - h]$ [23]. For $h > 2t$, all single particle states are localized. We think that this is an interesting model to study MBL because by tuning h one can tune the fraction of delocalised to localized single particle states in the non-interacting system and analyze how localized and delocalised states interact with each other. Also experimentally it is more easily realizable than a

model with fully random potential [26]. We study this model for $h < 2t$ as well as for $h > 2t$ using exact diagonalisation for various parameter values and analyze how localized and extended (or weakly localized) single particle states interact resulting in many-body mobility edge.

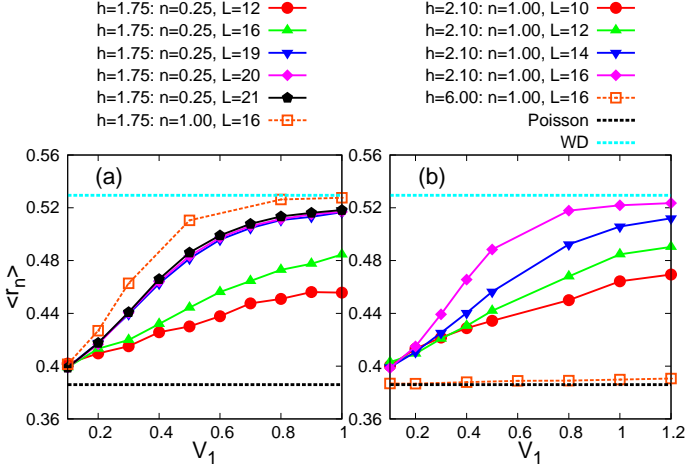


FIG. 2: Plot of $\langle r \rangle$ averaged over the entire spectrum vs V_1 for various system sizes. Left panel shows the results for $h = 1.75t < h_c$. Full curves show data for doped case with $\rho = 0.25$ for various L values. $\langle r \rangle$ increases with L as well as with V_1 approaching the WD value for $V_1 \sim t$. Note that for a given L , $\langle r \rangle$ for the half filled case is much larger than the corresponding values for $\rho = 0.25$ case and is closer to the WD value. The right panel shows $\langle r \rangle$ data for $h > h_c$ case. For $h = 2.1t$ for most of the values of V_1 in weak to intermediate regime, $\langle r \rangle$ is much below the value for WD distribution. Only for $V_1 \sim t$ $\langle r \rangle$ starts approaching WD value. On the other hand for $h = 6t \gg h_c$, $\langle r \rangle \sim 0.386$ for all the values of V_1 studied indicating that all the many body states are localized even in the presence of interaction.

RESULTS

The results described in the following sections are obtained by solving the model in Eq. 2 using exact diagonalization on finite size chains with open boundary conditions. Everywhere we choose $\alpha = \frac{\sqrt{5}-1}{2}$ and $n = 0.5$. We present results for $h = 1.75t$ for which single particle spectrum has a mobility edge as well as for $h = 2.1t$ and $6t$ for which all single particle states are localized. For $h = 1.75t$, we present results for the half filled case, i.e. with particle density $\rho = 1$ as well as doped case with $\rho = 0.25$. The phase diagram shown in Fig. 1 has been obtained on the basis of analysis of various quantities namely, energy spacing statistics, normalized participation ratio, Shannon entropy, Renyi entropy and ETH. Below we describe our results for each of these one by one.

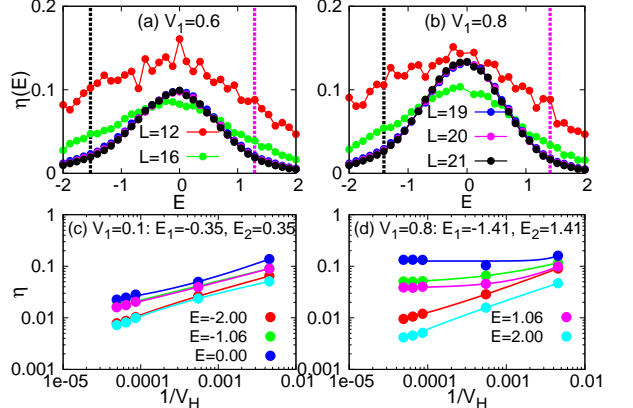


FIG. 3: Energy resolved NPR $\eta(E)$ vs the energy density E for $h = 1.75t$ and $\rho = 0.25$ for various values of L . In the middle of the spectrum $\eta(E)$ increases with increase in L while in the low and high energy ends of the spectrum, $\eta(E)$ decreases with increase in L indicating a crossover from localized to delocalised regime. The bottom panel shows the scaling of $\eta(E)$ vs $1/V_H$. For $V_1 = 0.1t$, for all the values of energy density (except for a few with $E \sim 0$), $\eta(E) \sim b * V_H^{-c}$ and hence vanishes in the thermodynamic limit indicating their localized nature. For $E = 0$, $\eta(E) \sim a + b * V_H^{-c}$ with a non zero value of a indicating the delocalised nature of $E = 0$ state. On increasing V_1 more many body states get delocalised as indicated in the right bottom panel for $V_1 = 0.8t$. Here $\eta(E) \rightarrow a \neq 0$ for $E = 0, \pm 1.06$ while for $E = \pm 2.06t$, $\eta(E)$ vanishes in the thermodynamic limit. This determines characteristic energies E_1 and E_2 such that many body states with $E < E_1$ and $E > E_2$ are localized while the intermediate states with $E_1 < E < E_2$ are delocalised. In the top panel we have shown E_1 and E_2 as dashed bars of black and pink color. This data is obtained by binning data for various configurations (50-100) over a bin size of $dE = 0.08t$ around an energy E .

Energy level spacing statistics

A convenient measure to differentiate between the localized and extended states is based on study of spectral statistics using tools from random matrix theory [27]. The distribution of energy level spacings is expected to follow Poisson statistics for many body localized phase while it follows Wigner-Dyson statistics for the ergodic phase. This is based on the intuition that in a localized phase, states which are close in energy live very far in the configuration space to be mixed by the kinetic energy and therefore the level repulsion is suppressed in the localized phase resulting in Poisson statistics for level spacings. On the other hand in an ergodic phase, disorder lifts degeneracies resulting in strong level repulsion leading to Wigner-Dyson statistics. Following [5], we calculate the ratio of successive gaps in energy levels $r_n = \frac{\min(\delta_n, \delta_{n+1})}{\max(\delta_n, \delta_{n+1})}$ with $\delta_n = E_{n+1} - E_n$ at a given eigen energy E_n of the Hamiltonian in Eq. 2 to discriminate between the two phases. For a Poissonian distribution, the disorder aver-

aged value of r is $2\ln 2 - 1 \approx 0.386$; while for the Wigner surmise of Gaussian orthogonal ensemble (GOE) mean value of $r \approx 0.5295$.

Fig. 2 shows the plot of average r vs the interaction strength V_1 for various system sizes. This data is obtained from r_n averaged over the entire energy spectrum for a given configuration of quasi-periodic potential and then averaged over 50-100 independent configurations obtained by varying ϕ . For $h = 6t$, $\langle r \rangle$ is close to Poisson value for all values of interactions indicating the presence of a MBL phase. But both, for $h = 1.75t$ with particle density 0.25 and $h = 2.1t$ with half-filling, $\langle r \rangle$ is close to the Poisson value for very small values of V_1 . $\langle r \rangle$ increases with system size L and starts approaching the Wigner-Dyson value for large V_1 values. But for most of the range of interactions, $\langle r \rangle$ is somewhere in between the two values, indicating that different parts of the energy spectrum might have different behaviour such that the average is neither close to the Poisson limit nor to the WD limit. Note that for $h = 1.75t$ at half filling, $\langle r \rangle$ is larger than its value for the quarter filled case and approaches wigner-dyson value for weaker strength of V_1 indicating that many body states for $h < h_c$ half-filled system are more extended than the states for the quarter filled case.

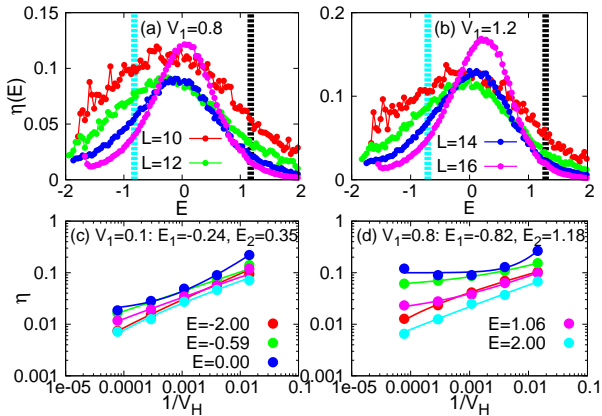


FIG. 4: Same as in Fig. 3 for $h = 2.1t$ half filled case. Bin size used here is $dE = 0.04t$.

Normalized Participation ratio in Fock space(NPR)

To decide whether a many-body state is localized or not, we calculate the NPR which is defined as

$$\eta(E) = \frac{1}{\langle \sum_{i,n} |\Psi_n(i)|^4 \delta(E - E_n) \rangle_C V_H} \quad (3)$$

where $\Psi_n(i)$ is an eigenfunction (normalized) with eigenvalue E_n of the Hamiltonian in Eq. 2, V_H is the volume of the Fock space, and $\langle \rangle_C$ indicates the configuration averaging. In our numerical calculation of $\eta(E)$, we replace

the delta function by a box distribution of finite width dE around energy density $E = E_n/N_p$ where N_p is the number of particles in the system. $\eta(E)$ represents the fraction of configuration space participating in a many-body state of energy E . For delocalised states, $\eta(E)$ is of order $O(1)$ while for states showing MBL, $\eta(E)$ decreases with increase in the system size and vanishes in the thermodynamic limit.

Fig. 3 shows the $\eta(E)$ vs E for $h = 1.75t$ doped case ($\rho = 0.25$). For very low and high energy states, $\eta(E)$ decreases as the system size increases while for states in the middle of the band $\eta(E)$ increases slightly with the system size [28]. This clearly shows that there is a difference in the behaviour of many body states across the spectrum. States in the middle of the spectrum are delocalised and do not show MBL. To see clearly whether the states at the bottom and top of the many body spectrum are localized, we did scaling of $\eta(E)$ w.r.t $1/V_H$ as shown in the bottom panel of Fig. 3. For delocalised states $\eta(E) \sim a + b(1/V_H)^c$ while for the states showing MBL $a = 0$. This is clearly visible on the log scale plots in the bottom panel of Fig. 3. Extrapolated values of $\eta(E)$ are shown in the density plot of Fig. 1. From the extrapolated values, we obtained energy densities E_1 and E_2 (shown as black and pink lines in the top panel of Fig. 3) such that $\eta(E) \rightarrow 0$ in the thermodynamic limit for states with $E < E_1$ and $E > E_2$ while it is finite for $E_1 < E < E_2$ indicating the presence of a mobility edge in the many body spectrum. Even for $h = 2.1t$ we get a similar picture from the analysis of NPR. Here since all single particle states are localized for $V_1 = 0$, all the many body states also show MBL. But for non zero V_1 states in the middle of the many body spectrum gets delocalised having finite value of $\eta(E)$ in the thermodynamic limit. This happens because $h = 2.1t$ is very close to h_c and some of the single particle states are very weakly localized. In Fig. 4 we have shown the corresponding data for $h = 2.1t$. The mobility edges E_1 and E_2 are shown by curves joining full dots in the phase diagram of Fig. 1.

Shannon Entropy

We also calculate Shannon entropy for every eigenstate $S(E_n) = -\sum_{i=1}^{V_H} |\Psi_n(i)|^2 \ln |\Psi_n(i)|^2$. Clearly for a many body state which gets contribution from all the basis states in the Fock space (and is normalized) $S(E_n) \sim \ln(V_H)$ and thus $f(E) = \exp(S(E_n))/V_H \sim 1$ while for a localized state which gets significant contribution only from some of the basis states, say N_l , in the Fock space, then $f(E) = \exp(S(E_n))/V_H \sim N_l/V_H$ vanishing to zero in the thermodynamic limit. Fig. 5 shows the plot for $f(E)$ vs E for various system sizes for $h = 1.75t$ doped case. Though for very small V_1 , $f(E)$ decreases with increasing system sizes for all values of E , the extrapolated value of f in the thermodynamic limit is

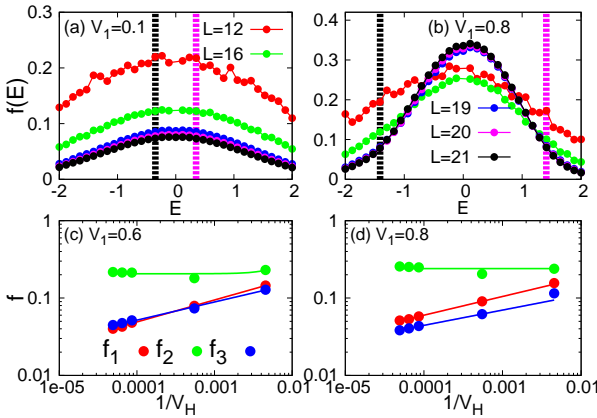


FIG. 5: $f(E) = \exp(S(E_n))/V_H$ (averaged over a bin of size $dE = 0.08t$) vs the energy density E for $h = 1.75t$ and $\rho = 0.25$. As shown in the top right panel, $f(E)$ increase with L for states in the middle of the spectrum while it decreases with L for states on the top and bottom of the spectrum, similar to NPR. Though for small values of interaction strength this pattern is not clear as shown in the top left panel for $V_1 = 0.1t$ where it seems $f(E)$ decreases with L for all E states. The bottom panel shows scaling of f_1 which is $f(E)$ averaged over all $E < E_1$, f_3 which is $f(E)$ averaged over $E > E_2$ and f_2 which is $f(E)$ averaged for $E_1 < E < E_2$. Both for $V_1 = 0.1t$ and $V_1 = 0.8t$, f_1 and f_2 vanish in the thermodynamic limit while f_2 stays finite indicating the delocalised nature of states in the middle region of the spectrum.

not zero for all E values. The bottom panel shows scaling of $f_{1,2,3}$ which are obtained by averaging $f(E)$ over three regions of the spectrum, namely, $E < E_1$, $E_1 < E < E_2$ and $E > E_2$. In close analogy to the NPR, f_2 is finite in the thermodynamic limit while f_1 and f_3 vanish indicating again the crossover from MBL to delocalised nature of states across the spectrum. A similar picture emerges for $h = 2.1t$ half filled case where also from the analysis of Shannon entropy we concluded that there is a many-body mobility edge in this model. Details of this are presented in the supplemental material [29]

Comparison of $h < h_c$ doped and half-filled case

Before we present our analysis of the entanglement entropy, we would like to compare the $h < h_c$ half filled case and the doped case based on our current analysis of NPR and Shannon entropy. So far we presented effect of interaction on system where in the non-interacting case Fermi energy lies below the single particle mobility edge E_c . Thus not only the states below the Fermi energy are localized, but many of states above it are localized too. In such a scenario, one of course expects the many body ground state and some of the excited states to show localization which already hints towards the presence of a many-body mobility edge in this system. Our nu-

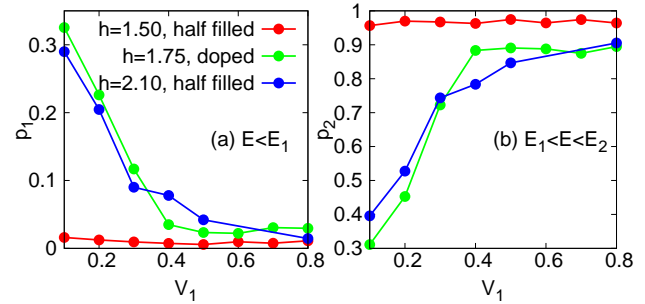


FIG. 6: Fraction of states vs V_1 in the localized and delocalised sector of the spectrum based on NPR analysis. Left panel shows the fraction for the localized sector on the low energy density side for $h < h_c$ as well as for $h > h_c$. Note that for $h < h_c$ doped case ($h = 1.75t$, $\rho = 0.25$), there is a finite fraction of many body states which show localization while for half filled $h < h_c$ case (e.g. $h = 1.5t$, $\rho = 1$), fraction of states in the localized sector of the many body spectrum is vanishingly small. For $h > h_c$ even at $\rho = 1$, there is a finite fraction of states in the localized sector. Right panel shows the results for fraction in the middle part of the spectrum which is delocalized.

merical study, presented above, demonstrated that even in the presence of interactions, of weak to intermediate strength, there is a mobility edge $E_{1,2}$ which separates the many body states (below E_1 and above E_2) showing MBL from the states which are delocalised. As the interaction strength increases more many body states in the middle of the spectrum get delocalised. Now consider the half filled case for $h < h_c$. Though in the non-interacting case there are mobility edges $\pm E_c$, but the Fermi energy is now in the middle of delocalised band. Though some of states below Fermi energy are localized, but states near the Fermi energy are all extended making this system metallic. In this case, turning on interactions should not make this system an insulator due to localization. Thus on physical ground, we do not expect either the many body ground state or any of higher energy state to show MBL in this case in the presence of interactions. But if one does finite size analysis of NPR and Shannon entropy, one might see $\eta(E)$ or $f(E)$ vanishing in the thermodynamic limit for $E < E_1$ and $E > E_2$ just like the doped case. We calculate the fraction of states below E_1 , above E_2 and in the intermediate energy regime for further analysis. For every configuration, we count number of energy states for a given L below E_1 and divide it by the total number of states V_H . We further average it over independent configurations and get p_1 . Similarly we obtain p_2 and p_3 which satisfy for any value of parameter set $\sum_i p_i = 1$. Fig. 6 shows the fraction of states for $h = 1.75t < h_c$ as a function of the interaction strength for the doped as well as the half-filled case. We clearly see that p_1 for the half filled case is vanishingly small

and is much smaller than the value for the doped case supporting our physical picture that there is no MBL for $h < h_c$ half filled case while there is a many body mobility edge for $h < h_c$ doped case. We have also shown for comparison the fraction of states for $h = 2.1t > h_c$ case at half filled where the fraction of states in the localized regime is finite and decreases with the interaction strength indicating a MBL to delocalization transition.

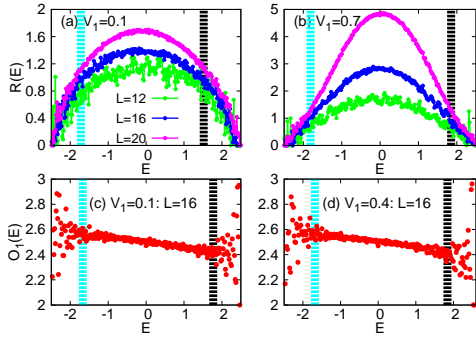


FIG. 7: Top panel shows energy resolved $R(E)$ vs E for $h = 1.75t$ and $\rho = 0.25$ for various values of L . There is a characteristic energy \tilde{E}_1 below which $R(E)$ is same for all L values within numerical error and same holds true for $E > \tilde{E}_2$. But for the intermediate states $\tilde{E}_1 < E < \tilde{E}_2$, $R(E)$ shows volume scaling law and increases with L indicating its ergodic nature. The ergodic regime increases with increase in V_1 as shown in the right panel for $V_1 = 0.7t$. The bottom panel shows expectation value of \hat{O} , which is the sum of number operators over subsystem A, vs E . Again below the characteristic energy which is close to \tilde{E}_1 , $\langle \hat{O} \rangle$ shows large fluctuations in its value for near by eigenstates and same holds true for $E > \tilde{E}_2$. But for the intermediate regime $\tilde{E}_1 < E < \tilde{E}_2$, fluctuations of $\langle \hat{O} \rangle$ among nearby energy states is small indicating its thermal nature. This data is obtained by binning over a bin in energy of size $dE = 0.02t$.

Entanglement Entropy

Entanglement entropy (EE) characterizes how information spreads from one part of the system to another and is a useful tool to distinguish between the ergodic and many-body localized phases. We divide the lattice into two subsystems A and B of sites $L/2$ and calculate the energy resolved Renyi entropy $R(E_n) = -\log[Tr_A \rho_A(E_n)^2]$ where ρ_A is the reduced density matrix obtained by integrating the total density matrix $\rho_{total}(E_n) = |\Psi_n\rangle\langle\Psi_n|$ over the degree of freedom of subsystem B. EE is expected to obey the volume law of scaling $R \sim L^d$ in the ergodic phase while the EE is suppressed for the MBL phase showing an area law scaling $R \sim L^{d-1}$ [21]. Here d is the physical dimension of the system.

Fig. 7 shows $R(E)$ which is obtained from $R(E_n)$ by binning over an energy bin dE around energy E and averaging over 50-100 configurations. For $E < \tilde{E}_1$, $R(E)$ is

same for various system sizes indicating that the many body states in this energy regime are localized with $R(E)$ obeying area law ($R(E) \sim L^0$). Same is true for many body states at the top of the spectrum with $E > \tilde{E}_2$, while for many-body states in the middle of the spectrum $\tilde{E}_1 < E < \tilde{E}_2$, $R(E) \sim L$ indicating their delocalised nature. As the strength of the interaction increases, the region of delocalised states increases. We would like to emphasize that this picture is qualitatively consistent with what we obtained from the analysis of NPR and Shannon entropy though values of $\tilde{E}_{1,2}$ are little off from $E_{1,2}$ obtained earlier, which can be seen clearly in Fig. 1. In Fig. 1, curves passing through full circles represent $E_{1,2}$ while curves passing through hexagons represent $\tilde{E}_{1,2}$. We conclude that the earlier analysis overestimates the region of localized states [30].

We would like to compare results for $h < h_c$ doped case with that for the half filled case for EE as well. Fig. 8 shows scaling of R vs L in three sectors of the many body spectrum obtained on the basis of NPR analysis for $h = 1.5t$ half filled case. We obtained $R_{1,2,3}$ by averaging $R(E)$ over energy density belonging to three sectors obtained by NPR analysis. Interestingly, R_1 and R_3 increases much slowly with L compared to R_2 . Combining this result with the fact that in a big enough system there are no states below E_1 and above E_2 , we conclude that for $h < h_c$ half filled case, the system remains delocalised with EE obeying volume law of scaling for all the many body states and for all values of the interaction strength.

We also calculated EE for $h = 2.1t$ half filled case as well and saw clear indications of ME, details of which are given in Fig. 9.

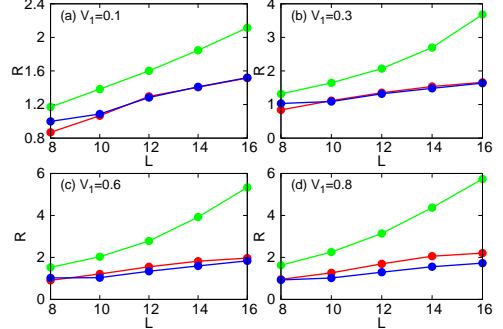


FIG. 8: Scaling of Renyi entropy vs L for $h = 1.5t$ at half filling. As explained in the text $R_{1,2,3}$ are obtained by averaging $R(E)$ over three sectors of the many body spectrum obtained on the basis of NPR analysis. Different panels show results for different values of V_1 . In all cases, R_1 and R_3 increase very slowly with L while R_2 shows a clear volume law scaling.

Eigenstate Thermalisation Hypothesis

In this section we check for the ETH in various parameter regimes by calculating expectation value of the number operator on subsystem A which has $L/2$ sites w.r.t various eigenstates. We define $\hat{O} = \sum_{i=1}^{L/2} \hat{n}_i$ where \hat{n}_i is the number operator for spinless fermions at site i . For every eigenstate, we calculate the expectation value $\langle O \rangle_n = \langle \Psi_n | \hat{O} | \Psi_n \rangle$ and from their obtained $O(E)$ which is obtained by averaging $O(E_n)$ over all E_n values which belong to the bin $E \pm dE$. This is further averaged over many independent configurations. For an ergodic phase, $O(E)$ does not have large fluctuations for nearby eigenstates.

Fig. 9 shows $O(E)$ as a function of E for $h = 1.75$ doped case. We observe that for states with $E < \tilde{E}_1$ and $E > \tilde{E}_2$, many body system is not thermal showing violation of ETH while for $\tilde{E}_1 < E < \tilde{E}_2$, system is ergodic and obeys ETH. Further as it is clear from Fig 7, that $\tilde{E}_{1,2} \sim \tilde{E}_{1,2}$ within numerical error indicating that the transition from non-thermal to thermal phase occurs at the same energy at which the EE shows transition from area to volume law of scaling. This is clearly shown in the Fig. 1 where curves joining triangles show $\tilde{E}_{1,2}$. We did similar analysis for $h = 2.1t$ half filled case as well and the result is shown in Fig. 9.

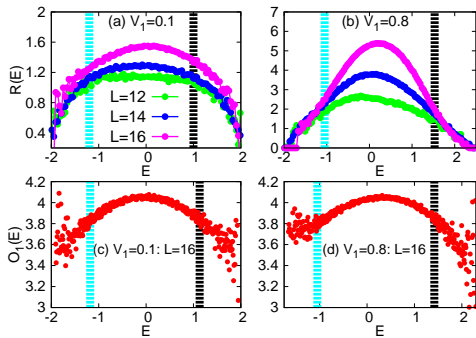


FIG. 9: Same as in Fig. 7 for $h = 2.1t$ and $\rho = 1$. This data is obtained by binning over a bin in energy of size $dE = 0.01t$.

CONCLUSIONS

In summary we have analysed MBL in an interacting 1-d model of spinless fermions in the presence of a quasi-periodic potential. If there is a single particle ME in the noninteracting system, and the particle density is such that the ground state and many of excited states are localized, then even in the presence of interactions system has a many body ME. MBL states live on the low and very high energy part of the spectrum while the middle

of the spectrum has delocalised states. If in the noninteracting case with $h < h_c$, the particle density is half filled such that the ground state is extended, then even in the presence of interactions all the many body states remain delocalised. Interactions can also lead to delocalisation of some parts of the many body spectrum even when all the single particle states are localized. This happens when a part of single particle states are weakly localized. Further, our numerical results demonstrate that the transition from area to volume law scaling of EE are accompanied by non-thermal to thermal transition based on the analysis of ETH and the analysis of normalized participation ratio in Fock space overestimates the region of MBL phase.

ACKNOWLEDGEMENTS

S. N would like to acknowledge Kausik Das (SINP) for computational help.

- [1] P. W. Anderson, Phys. Rev. **109**, 1492 (1958).
- [2] E. Abrahams, P. W. Anderson, D. C. Licciardello, and T. V. Ramakrishnan, Phys. Rev. Lett. **42**, 673 (1979).
- [3] P. A. Lee and T. V. Ramakrishnan, Rev. Mod. Phys. **57**, 287 (1985).
- [4] D. M. Basko, I. L. Aleiner, and B. L. Altshuler, Ann. Phys. (Amsterdam), **321**, 1126 (2006).
- [5] V. Oganesyan and D. A. Huse, Phys. Rev. B **75**, 155111 (2007).
- [6] A. Pal and D. A. Huse, Phys. Rev. B **82**, 174411 (2010).
- [7] R. Nandkishore and D. A. Huse, Ann. Rev. Cond. Matt. Phys. **6**, 15 (2015).
- [8] E. Altman and R. Vosk, Ann. Rev. Cond. Matt. Phys. **6**, 383 (2015).
- [9] J. M. Deutsch, Phys. Rev. A **43**, 2046 (1991).
- [10] M. Srednicki, Phys. Rev. E **50**, 888 (1994).
- [11] M. Rigol, V. Dunjko, and M. Olshanii, Nature (London), **452**, 854 (2008).
- [12] D. A. Huse, R. Nandkishore, and V. Oganesyan, Phys. Rev. B **90**, 174202 (2014).
- [13] R. Modak, S. Mukerjee, E. A. Yuzbashyan, and B. S. Shastry, arXiv:1503.07019.
- [14] M. Serbyn, Z. Papic, and D. A. Abanin, Phys. Rev. Lett. **111**, 127201 (2013).
- [15] V. Ros, M. Mueller, and A. Scardicchio, Nucl. Phys. B **891**, 420 (2015).
- [16] S. Bera, H. Schomerus, F. H-Meisner, and J. H. Bardarson, Phys. Rev. Lett. **115**, 046603 (2015).
- [17] T. Enss, F. Andraschko, J. Sirker, arXiv:1608.05733.
- [18] V. Ros and M. Mueller, arXiv:1608.06225.
- [19] S. Iyer, V. Oganesyan, G. Refael, and D. A. Huse, Phys. Rev. B **87**, 134202 (2013).
- [20] R. Modak and S. Mukerjee, Phys. Rev. Lett. **115**, 230401 (2015).

- [21] X. Li, S. Ganeshan, J. H. Pixley, and S. D. Sarma, Phys. Rev. Lett. **115**, 186601 (2015).
- [22] S. Aubry and G. Andre, Ann. Isr. Phys. Soc. **3**, 18 (1980).
- [23] S. Ganeshan, J. H. Pixley, and S. D. Sarma, Phys. Rev. Lett. **114**, 146601 (2015).
- [24] J. A. Kjall, H. H. Bardarson, and F. Pollmann, Phys. Rev. Lett. **113**, 107204 (2014).
- [25] D. J. Luitz, N. Laflorencie, F. Alet, Phys. Rev. B **91**, 081103(R) (2015).
- [26] M. Schreiber, S. S. Hodgmann, P. Bordia, H. P. Lschen, M. H. Fischer, R. Vosk, E. Altman, U. Schneider, and I. Bloch, Science **349**, 842 (2015).
- [27] M. L. Mehta, *Random Matrices* (Academic, Boston, 1991).
- [28] Data for $L = 12$ does not follow this trend probably because of too small dimension of the Hilbert space.
- [29] See supplementary material.
- [30] T. Devakul and R. R. P. Singh, Phys. Rev. Lett. **115**, 187201 (2015).